Journal Pre-proof

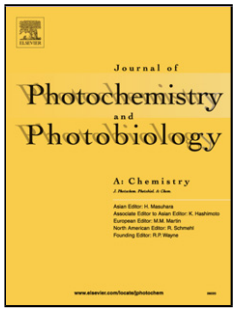

A new "off-on-off" sensor for sequential detection of Al^{3+} and Cu^{2+} with excellent sensitivity and selectivity based on different sensing mechanisms

Yuankang Xu, Lei Yang, Hanyu Wang, Yanxia Zhang, Xiaofeng Yang, Meishan Pei, Guangyou Zhang

PII: S1010-6030(19)31933-1

DOI: https://doi.org/10.1016/j.jphotochem.2020.112372

Reference: JPC 112372

To appear in: *Journal of Photochemistry & Photobiology, A: Chemistry*

Received Date: 12 November 2019

Revised Date: 24 December 2019

Accepted Date: 11 January 2020

Please cite this article as: Xu Y, Yang L, Wang H, Zhang Y, Yang X, Pei M, Zhang G, A new "off-on-off" sensor for sequential detection of Al^{3+} and Cu^{2+} with excellent sensitivity and selectivity based on different sensing mechanisms, *Journal of Photochemistry and amp; Photobiology, A: Chemistry* (2020), doi: https://doi.org/10.1016/j.jphotochem.2020.112372

A new "off-on-off" sensor for sequential detection of Al^{3+} and Cu^{2+} with excellent sensitivity and selectivity based on different sensing mechanisms

Yuankang Xu[a], Lei Yang[b,*], Hanyu Wang[a], Yanxia Zhang[a], Xiaofeng Yang[a], Meishan Pei[a] and Guangyou Zhang[a,*]

[a] School of chemistry and chemical engineering, University of Jinan, Jinan 250022, China, E-mail address: chm_zhanggy@ujn.edu.cn.

[b] Henan Sanmenxia Aoke Chemical Industry Co. Ltd., Sanmenxia 472000, China. E-mail address: 275665616@qq.com.

***Corresponding author**: Guangyou Zhang, E-mail address: chm_zhanggy@ujn.edu.cn. Lei Yang, E-mail address: 275665616@qq.com.

Graphical abstract

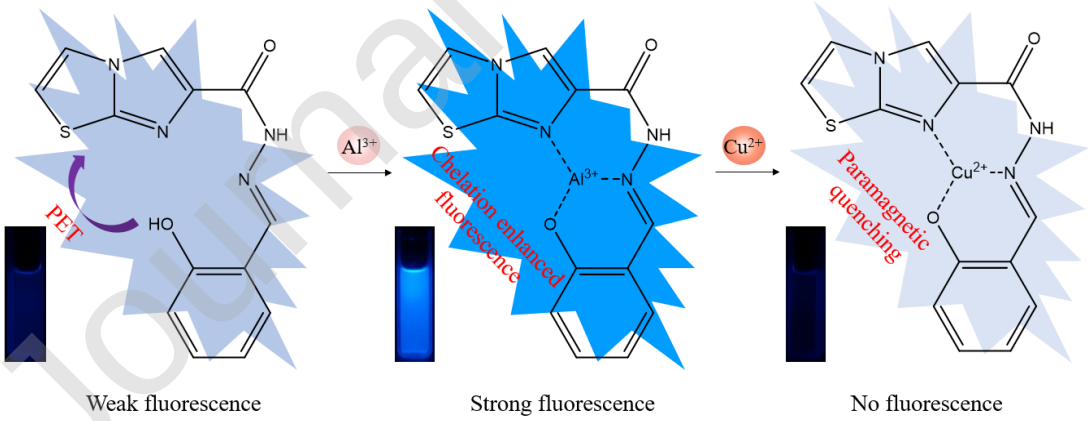

Highlights

- A new simple fluorescence sensor (**X**) was designed and synthesized based on salicylaldehyde and imidazo[2, 1-*b*]thiazole.
- **X** could be used as "off-on-off" sensor for sequential detection of Al^{3+} and Cu^{2+} with excellent sensitivity and selectivity based on different sensing mechanisms
- The detection limits of sensor for Al^{3+} and Cu^{2+} were calculated to be 3.1×10^{-10} M and 9.8×10^{-11} M, respectively.
- The optimized structure and energy calculations of **X**, **X**[Al^{3+}] and **X**[Cu^{2+}] were obtained by Gaussian 09 to prove the binding mode and sensing mechanism.
- The sensor successfully detected Al^{3+} and Cu^{2+} in the real water sample with a satisfactory recovery and RSD values

Abstract

A new simple Schiff base, (E)-N'-(2-hydroxybenzylidene)imidazo[2,1-b]thiazole-6-carbohydrazide (**X**), was designed and synthesized based on salicylaldehyde and imidazo[2, 1-*b*]thiazole. **X** could be used as a sensor to identify Al^{3+} through a significant fluorescence enhancement because of CHEF and inhibition of PET process and then to detect Cu^{2+} through a highly efficient quenching behavior due to the paramagnetic quenching. The sensor showed a high selectivity for Al^{3+} and Cu^{2+} in methanol solution at pH = 5 and was not disturbed by other competing metal ions. Furthermore, based on the equation 3σ/slope, the detection limits of sensor for Al^{3+} and Cu^{2+} were calculated to be 3.1×10^{-10} M and 9.8×10^{-11} M, respectively. Additionally, the association constants of **X**[Al^{3+}] and **X**[Cu^{2+}] were also determined to be 2.3×10^{4} M^{-1} and 6.1×10^{4} M^{-1} on basis of Benesi-Hildebrand equation. In addition, the titration experiment of fluorescence and mass spectrometry showed that sensor was combined with Al^{3+} or Cu^{2+} both in 1:1 ratio. Moreover, the optimized structure and energy calculations of **X**, **X**[Al^{3+}] and **X**[Cu^{2+}] were obtained by Gaussian software based on the basis set of B3LYP/6-31G(d) and B3LYP/LANL2DZ. And, the sensor successfully detected Al^{3+} and Cu^{2+} in the real water sample with a satisfactory recovery (91.4 % - 107.1%) and RSD values (0.66 % - 1.91 %).

Keywords: Schiff base; Excellent detection limit; Different sensing mechanisms; Theoretical calculation; real water sample.

1. Introduction

In recent years, one of the hot areas is the detection and determination of metal ions like aluminum and copper with high sensitivity and selectivity due to their importance in biological, medical, environmental and industrial fields [1-3]. Aluminum, after oxygen and silicon, is the third most abundant element in the earth' crust (about 8%) and is characterized by good ductility and high melting point which has many applications in daily life, such as packaging materials, refractory materials and building materials [4-7]. According to the World Health Organization (WHO), the average daily human intake of aluminum is approximately 3-10 mg while the permissible limit is 7.4×10^{-6} M in drinking water [8]. However, aluminum is not one of the essential metal ions for the human body, and its excessive absorption could lead to a various of diseases including myopathy, Alzheimer's disease and Parkinson's disease [9-12]. Furthermore, influenced by acid rain and industrial acid wastewater discharge, the content of aluminum in soil was up surged with the increase of acidity, which restricts the growth and development of plants [13-15]. Copper is third abundant and essential trace element in human body, next to iron and zinc, which could participate in the metabolism of all sorts of enzymes and maintain normal hemopoietic function and the health of central nervous system [16-19]. In the human body, the normal concentration of copper is about 15.6 - 23.6 μM [20]. The imbalances in capper concentration could lead to various diseases, such as Alzheimer's disease, Huntington disease and Wilson's disease [21-23]. Meanwhile, plants could experience symptoms of victimization including physiological arrest, stunted development and even death when copper accumulate in a certain amount [24-26]. Thus, the detection of aluminum and copper with effectivity and selectivity is of great significance for bioscience and environmental sciences.

Till now, some high-efficiency fluorescent sensors with excellent optical response for aluminum or copper have been developed and gradually replaced the traditional monitoring methods

(atomic absorption spectrometry, atomic emission spectrometry and inductively coupled plasma mass spectrometry), which become a new monitoring method with simple operation, high sensitivity and selectivity [27-30]. However, based on respective sensing mechanisms like photoinduced electron transfer (PET), chelation enhanced fluorescence (CHEF), paramagnetic quenching and others, some of fluorescent sensors could only detect a single metal ion, aluminum or copper, which greatly limits their application [31-34]. In contrast, the multifunction sensor which could detect multiple metal ions based on different mechanism exhibited many advantages, including multiplicity, simple operation and so on [35, 36]. Nowadays, some sensors have been designed and synthesized, which could detect both aluminum and copper [37]. Unfortunately, the sensors that have been reported still have many shortcomings, including poor sensitivity and susceptibility to interference from other ions. Moreover, there are few articles that could give a comprehensive description and exploration of the sensing mechanism of multi-function sensor for aluminum and copper [38]. As a result, there is still an urgent need to design and synthesize an ultra-sensitive sensor to accurately detect aluminum and copper based on the coordinated control of multiple sensing mechanisms.

Recently, a series of fluorescent sensors based on imidazo[2, 1-*b*]thiazole were designed and synthesized by our group for different metal ions [39, 40]. As one of heterocyclic compounds, imidazo[2, 1-*b*]thiazole, has shown excellent optical properties and good identification ability like other commonly used fluorescent nuclei (rhodamine, naphthalimide and coumarin), suggesting that it could be used as a potential fluorophore [41-43]. In addition, salicylaldehyde was the most commonly used aldehydes for the synthesis of Schiff base, which provide hydroxyl groups to increase the ability of binding metal ions [44, 45]. In this report, a new Schiff base, (E)-N'-(2-hydroxybenzylidene)imidazo[2,1-b]thiazole-6-carbohydrazide (**X**), was prepared by linking salicylaldehyde and imidazo[2, 1-*b*]thiazole with a C=N bond. As expected, the sensor **X** exhibited a weak fluorescence intensity based on PET process. After binding with Al^{3+}, a new complex, **X**[Al^{3+}], was formed and displayed a strong fluorescence intensity due to the inhibition of PET process. Furthermore, the complex **X**[Al^{3+}] could be further used as a new sensor for Cu^{2+} based on the paramagnetic quenching, showing efficient fluorescence quenching behavior. In a word, **X** could be used as a sensor for Al^{3+} and Cu^{2+} with excellent sensitivity and selectivity in methanol buffer

solution (methanol/H_2O = 9/1, 10 mM tris, pH = 5.0) based on the coordinated control of multiple sensing mechanisms.

2. Experimental section

2.1. Materials and sample preparation

All reagents and solvents were commercially available AR and CP and were used without any treatment. All metal ionic solution are corresponding chloride and sulfate solutions, including $AlCl_3$, $ZnCl_2$, Li_2SO_4, $CdCl_2$, $CoCl_2$, $FeCl_3$, $MgCl_2$, $CrCl_3$, $MnCl_2$, AgCl, KCl, $CuCl_2$, $NiCl_2$, $HgCl_2$. Stock solutions of the metal ions mentioned above were prepared with a concentration of 0.03 M by distilled water. Stock solutions of Al^{3+} and Cu^{2+} were further prepared with a concentration of 0.03 M by tap water. The **X** was dissolved in methanol/H_2O (v/v = 9 : 1) buffer solution (10 mM tris, pH = 5.0) at room temperature with the concentration of 1×10^{-5} M.

2.2. Measurements

UV-vis spectra were obtained on a Shimadzu 3100 spectrometer. Fluorescence spectral data was recorded on an Edinburgh Instruments Ltd-FLS920 Fluorescence Spectrophotometer. Fluorescence measurements were recorded using excitation at 365 nm. The slits of excitation and emission were 10 nm and 5 nm, respectively. ^{1}H NMR measurement was performed on a Bruker AV III 400 MHz NMR spectrometer with tatramethysilane (TMS) as internal standard and DMSO as solvent. ^{13}C NMR spectra data was taken on a Bruker AV III 100 MHz NMR spectrometer with tatramethysilane (TMS) as internal standard and DMSO as solvent. Infrared spectral data was obtained on a Bruker Vertex 70 FT-IR spectrometer using samples as KBr pellets. Thin layer chromatography (TLC) analyses were performed to monitor all the reactions.

2.3. Calculation of quantum yield, detection limit and association constant

Quantum yield was calculated according to the following formula (1):

$$\Phi_u = \Phi_s \frac{F_u A_s n_u^2}{F_s A_u n_s^2}$$

Φ, *F*, *A*, and *n* represent the quantum yield, the integrated area under the corrected emission spectra, the absorbance intensity at the excitation wavelength and the refractive index of solvent, respectively. In addition, *s* refers to rhodamine B as the standard, and *u* refers to the target. The quantum yield (Φ) of rhodamine B dissolved in anhydrous ethanol is 0.97.

The detection limit of sensor for metal ions was calculated by the following formula (2):

$$DL = \frac{3\sigma}{S}$$

σ is the standard deviation of 10 times blank measurements and *s* is the slope between fluorescence intensity *versus* metal concentration.

The association constant between **X** and metal ions was calculated by the Benesi-Hildebrand eqn (3):

$$\frac{1}{F - F_0} = \frac{1}{M^{n+}} \times \frac{1}{K_a[F_{max} - F_0]} + \frac{1}{F_{max} - F_0}$$

where *F* is the fluorescence intensity of the **X**[M^{n+}] complex, which is in accordance with the concentration of M^{n+}. F_0 is the fluorescence intensity of free **X**. *F*max is the fluorescence intensity of **X**[M^{n+}] complex in the presence of the maximum concentration of M^{n+}.

2.4. Theoretical calculations

Density functional theory (DFT) structural optimizations were performed with the Gaussian 09 program. In all cases, the structures were optimized using the B3LYP functional and the mixed basis set 6-31+G (d) and LANL2DZ. Each structure was subsequently subjected to TD-DFT calculation using the B3LYP functional [39]. For all optimized structures, frequency calculations were performed to confirm the absence of imaginary frequencies. The molecular orbitals were visualized and plotted with the GaussView 5.0 program.

2.5. Synthesis and characterization of X

Compound **1** (ethyl imidazo[2,1-b]thiazole-6-carboxylate) and compound **2** (imidazo[2,1-b]thiazole-6-carbohydrazide) were prepared according to a previous report [40].

Synthesis of **(E)-N'-(2-hydroxybenzylidene)imidazo[2,1-b]thiazole-6-carbohydrazide** (**X**). imidazo[2,1-b]thiazole-6-carbohydrazide (210 mg, 1.15 mmol) and 2-hydroxybenzaldehyde (166 mg, 1.36 mmol) were added to 50 ml round bottom flask containing 15ml of ethanol. Then the mixture was stirred for 12 hours at room temperature until pale-yellow precipitate appeared. After the reaction, the pale-yellow precipitate was collected by filtration and washed with cold ethanol to obtain the pure solid **X**. Yield: 224 mg, 71.2 %. Ms (ESI): m/z = 287.07 $[M + H]^+$, 309.03 $[M + Na]^+$. FTIR (KBr, cm^{-1}): 3322 (N−H), 1670 (C=O). ^{1}H NMR (400 MHz, DMSO) δ 12.18 (s, 1H), 11.48 (s, 1H), 8.71 (s, 1H), 8.40 (s, 1H), 8.00 (d, *J* = 4.5 Hz, 1H), 7.44 (t, *J* = 5.6 Hz, 2H), 7.32 – 7.25 (m, 1H), 6.92 (t, *J* = 7.6 Hz, 2H). ^{13}C NMR (101 MHz, DMSO) δ 158.49, 158.01, 149.45, 149.13, 140.48, 131.66, 130.37, 120.71, 119.77, 119.09, 117.23, 116.92, 116.13.

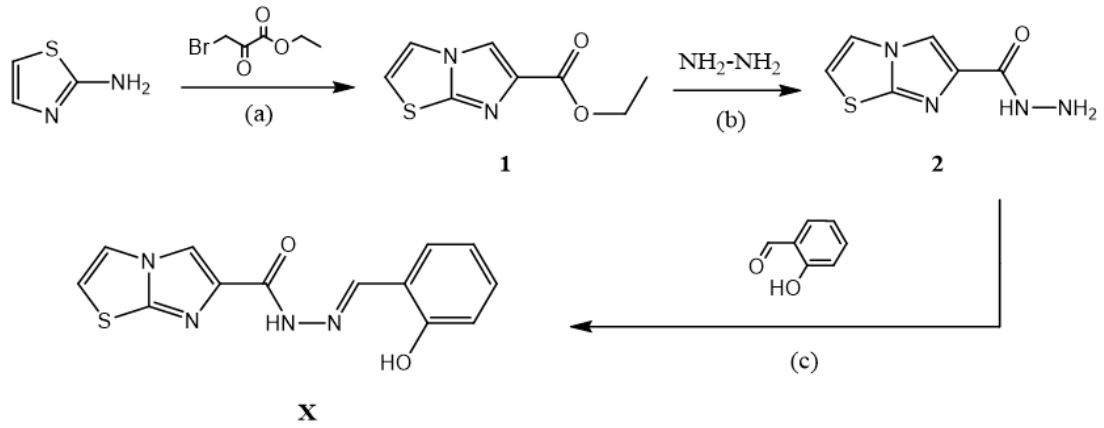

Scheme 1. Synthesis routes of **X**. Conditions: (a) THF/ethanol, r.t./refluxed, 20 h/4 h; (b) ethanol, r.t., overnight; (c) ethanol, r.t., 12 h.

3. Results and discussion

As shown in scheme 1, **X** was designed and synthesized in medium yield according to the synthetic route. Compound **1** (ethyl imidazo[2,1-b]thiazole-6-carboxylate) and compound **2** (imidazo[2,1-b]thiazole-6-carbohydrazide) were synthesized according to a previous report [40]. Then, **X** was synthesized by the reaction of Compound **1** and **2** with 71.2 % yield in ethanol and characterized by ^{1}H NMR (Fig. S1), ^{13}C NMR (Fig. S2), FTIR (Fig. S3), ESI-MS (Fig. S4). All of the data in the spectra were in good accordance with the structure.

3.1. The response time studies of X to Al^{3+}

First of all, the effect of response time on the fluorescence intensity of **X** was investigated in the presence of Al^{3+}. As shown in Fig. S5, upon addition of Al^{3+} (50 μM), the fluorescence intensity of **X** (1×10^{-5} M) at 455 nm gradually increased with time in methanol/H_2O buffer solution (v/v = 9/1, tris = 10 mM, pH = 5.0) under excitation wavelength of 365 nm. Obviously, the response time of **X** for Al^{3+} was less than 30 minutes. The fluorescence intensity reached the maximum and remained stable in the next 10 minutes, indicating the high reactivity of **X** for Al^{3+}. So, for the stability of the experiment and to get a good experimental result, 1 hour of complexation time was used in all experiments about Al^{3+}, which means that all samples should be stationary for 1 hour before testing.

3.2. The optical properties of X towards various metal ions

The sensing behavior of **X** toward various metal ions, including Al^{3+}, Cu^{2+}, K^{+}, Ag^{+}, Hg^{2+}, Cd^{2+}, Mn^{2+}, Li^{+}, Ni^{2+}, Fe^{3+}, Zn^{2+}, Cr^{3+}, Mg^{2+} and Co^{2+}, were investigated by fluorescence

spectroscopy in methanol/H_2O buffer solution (v/v = 9/1, tris = 10 mM, pH = 5.0). As shown in Fig. 1, as expected, the free **X** exhibited weak fluorescence intensity with a quantum yield of 0.035 under the excitation wavelength of 365 nm. When various metal ions (10 equiv.) were added to the system above, the fluorescence intensity at 445 nm increased sharply with Al^{3+}, showing a strong blue fluorescence (Φ = 0.64) which can be seen in the Fig. 1 insert. However, the fluorescence intensity still remained closed behavior with the addition of other metal ions. Meanwhile, the UV-vis spectrum of **X** for various metal ions (Al^{3+}, Cu^{2+}, K^{+}, Ag^{+}, Hg^{2+}, Cd^{2+}, Mn^{2+}, Li^{+}, Ni^{2+}, Fe^{3+}, Zn^{2+}, Cr^{3+}, Mg^{2+} and Co^{2+}) were also explored under the same condition. As shown in Fig. S6, the free **X** showed three absorbance bands at 288 nm, 299nm and 325nm, respectively. When various metal ions were added, some metal ions could also cause obvious change in absorption spectrum besides Al^{3+}, including Fe^{3+}, Ni^{3+}, Cu^{2+} and Co^{2+}. However, no noteworthy change in absorption bands could be observed upon addition of other metal ions. That is, **X** could be used as a sensor to detect of Al^{3+} by emission color changed.

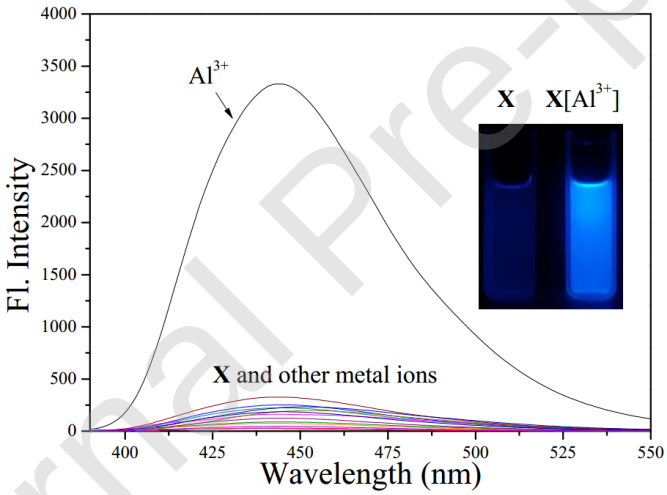

Fig. 1. Fluorescence spectra of **X** (10 μM) upon addition of various metal ions (10 equiv.) in methanol/H_2O buffer solution (v/v = 9/1, tris = 10 mM, pH = 5.0). Insert: the fluorescence intensity of X in the absence and presence of Al^{3+} under UV light of 365 nm.

3.3. The sensing of X for Al^{3+}

In order to further explore the sensing properties of **X** on Al^{3+}, the related fluorescence and UV-vis titration experiments were carried out in methanol/H_2O buffer solution (v/v = 9/1, tris = 10 mM, pH = 5.0). As shown in Fig. 2, the fluorescence intensity of **X** was weak at 445 nm, which could increase gradually as the concentration of Al^{3+} changed from 0 to 5 equiv. and tend to stabilize

when the concentration of Al^{3+} was greater than 5×10^{-5} M. As shown in Fig. S7, the fluorescence intensity of **X** had a good linear relationship (R^2 = 0.9833) with low level of Al^{3+}. Based on the fluorescence titration data, the detection limit of **X** for Al^{3+} was calculated to be 3.1×10^{-10} M by the equation 3σ/slope. Otherwise, the association constants of **X**[Al^{3+}] were also determined to be 2.3×10^4 M^{-1} on basis of Benesi-Hildebrand equation (Fig. S8). The UV-vis titration experiments were also performed in Fig. 3, with the gradual addition of Al^{3+} (0 to 10 equiv.), the absorbance bands at 288 nm, 299nm and 325nm displayed a lessening accompanied by appearance of new bands at 308nm, 322nm and 374nm, respectively. Distinctive isosbestic points were found at 262 nm, 304 nm, 326 nm and 347 nm, indicating that a stable complex (**X**[Al^{3+}]) was formed between **X** and Al^{3+}. As shown in Fig. 4, the job's plot showed 1:1 stoichiometry between the **X** and Al^{3+} because the maximum fluorescent intensity was centered at 0.5 M fraction. The ESI mass spectra of **X**[Al^{3+}] was also performed in Fig. S9, the peak at *m/z* 312.03 was attributed to [**X** + Al^{3+} - H^+]$^{2+}$ (calcd *m/z* 312.02). The titration results showed that **X** could be used as a sensor with excellent performance (including high sensitivity and stable binding ability) toward Al^{3+}.

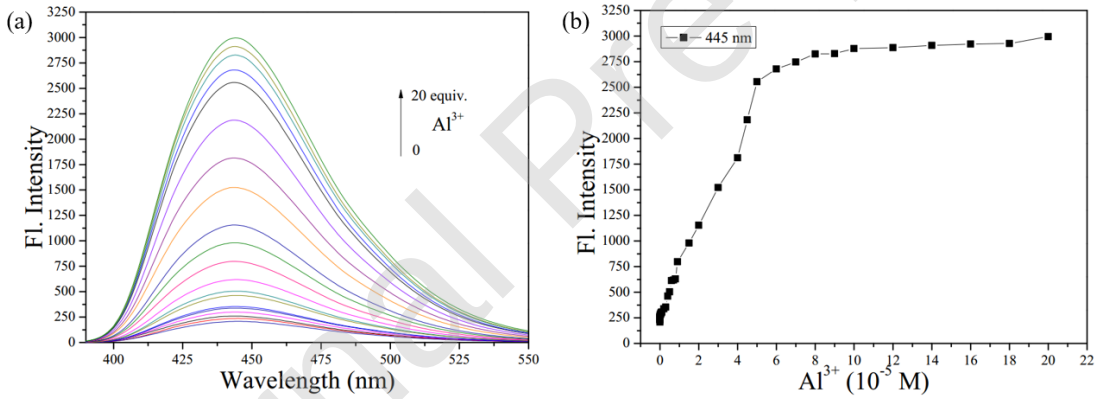

Fig. 2. Fluorescence emission spectra of **X** (10 μM) upon gradually addition of Al^{3+} (0 to 20 equiv.) in methanol/H_2O buffer solution (v/v = 9/1, tris = 10 mM, pH = 5.0).

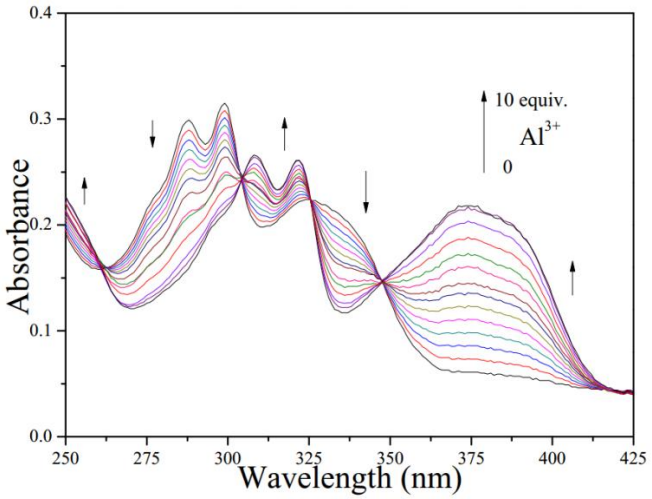

Fig. 3. Absorbance spectra of **X** (10 μM) upon gradually addition of Al^{3+} (0 to 10 equiv.) in methanol/H_2O buffer solution (v/v = 9/1, tris = 10 mM, pH = 5.0).

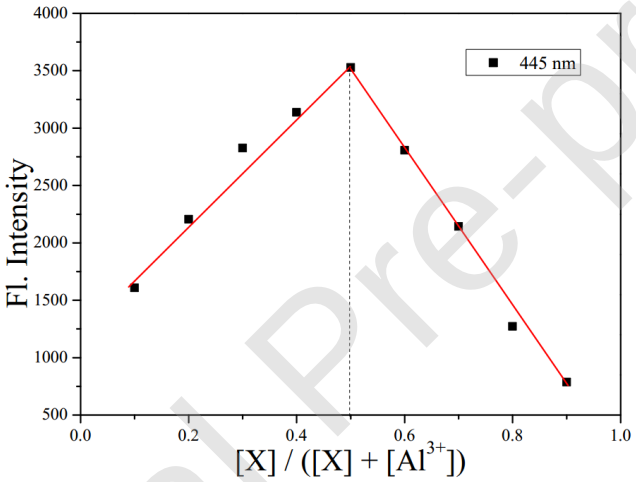

Fig. 4. Job's plot of **X** in methanol/H_2O buffer solution ([**X**] + [Al^{3+}] = 1.0 × 10^{-4} M).

3.4. Interference experiment with other metal ions

In order to explore the anti-interference ability of **X** as a sensor for Al^{3+}, the competition experiment was carried out in Fig. 5. For this purpose, **X** was mixed with Al^{3+} (10 equiv.) and then different interfering ions (Cu^{2+}, K^+, Ag^+, Hg^{2+}, Cd^{2+}, Mn^{2+}, Li^+, Ni^{2+}, Fe^{3+}, Zn^{2+}, Cr^{3+}, Mg^{2+} and Co^{2+}) were added separately. The results showed that the response of **X** to Al^{3+} were relatively low but still clearly detectable in the presence of Hg^{2+}, Ni^{2+}, Fe^{3+} and Co^{2+}. However, when addition of Cu^{2+}, the fluorescence intensity of X[Al^{3+}] system was completely quenched, displaying an efficient "turn-off" behavior [46, 47]. Consequently, **X** could be used as a sensor to selectively recognize Al^{3+} through obvious fluorescence enhancement without interference from most metal ions. And

the new complex **X**[Al^{3+}] form by **X** and Al^{3+} could be further used as an efficient quenching sensor for Cu^{2+}.

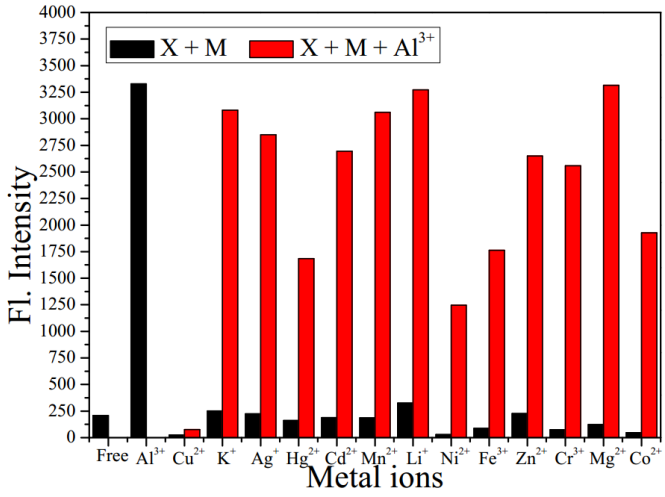

Fig. 5. Fluorescence response of **X** (10 μM) to different metal ions (10 equiv.) in the absence/presence of Al^{3+} (10 equiv.) in methanol/H_2O buffer solution (v/v = 9/1, tris = 10 mM, pH = 5.0). Black bar: **X** with Cu^{2+}, K^+, Ag^+, Hg^{2+}, Cd^{2+}, Mn^{2+}, Li^+, Ni^{2+}, Fe^{3+}, Zn^{2+}, Cr^{3+}, Mg^{2+} and Co^{2+}. Red: **X** with different metal ions in the presence of Al^{3+}.

3.5. The sensing of X[Al^{3+}] for Cu^{2+}

To gain insight into the sensing properties of X[Al^{3+}] for Cu^{2+}, the related fluorescence titration experiments were conducted by gradual addition of various concentrations of Cu^{2+} in methanol/H_2O buffer solution (v/v = 9/1, tris = 10 mM, pH = 5.0). Based on the above experiments, the fluorescence intensity of **X** was significantly enhanced when 10 equiv. of Al^{3+} were added. As shown in Fig. 6, the fluorescence intensity at 445 nm decreased gradually with the increased of Cu^{2+} (0 to 4 equiv.) under an excitation wavelength of 365 nm. Moreover, upon addition of lower than 2 equiv. of Cu^{2+}, the fluorescence intensity decreased drastically. However, the subsequent addition of 2 equiv. of Cu^{2+} had little effect on fluorescence intensity. This indicated that **X**[Al^{3+}] had excellent sensing behavior for Cu^{2+}. Therefore, as shown in Fig. S10, the change of fluorescence intensity (I_0 - I) at 445 nm was linearly proportional (R^2 = 0.9967) to the low concentration of Cu^{2+} (0 - 1 × 10^{-8} M). And the detection limit was calculated to be 9.8 × 10^{-11} M based on the equation 3σ/s, which was lower than many reported Cu^{2+} sensor [48-50]. Otherwise, the association constants of **X**[Cu^{2+}] were also determined to be 6.1 × 10^4 M^{-1} on basis of Benesi-Hildebrand equation (Fig. S11). The results of mass spectrometry titration in the presence of Cu^{2+} were shown in Fig. S12, the

peak at *m/z* 347.96 could be assigned to the complex [X + Cu^{2+} - H^+]$^+$ (calcd *m/z* 347.97), which proves that the complexation ratio between X and Cu^{2+} was 1:1. The competition experiment was shown in Fig. 7, the results indicated that **X**[Al^{3+}] could maintain the quenching sensing behavior for Cu^{2+} regardless of the presence or absence of other interfering ions (including K^+, Ag^+, Hg^{2+}, Cd^{2+}, Mn^{2+}, Li^+, Ni^{2+}, Fe^{3+}, Zn^{2+}, Cr^{3+}, Mg^{2+} and Co^{2+}). These results primarily indicated that the complex **X**[Al^{3+}] could be considered as a potential sensor for Cu^{2+} with excellent sensitivity and anti-interfere capability.

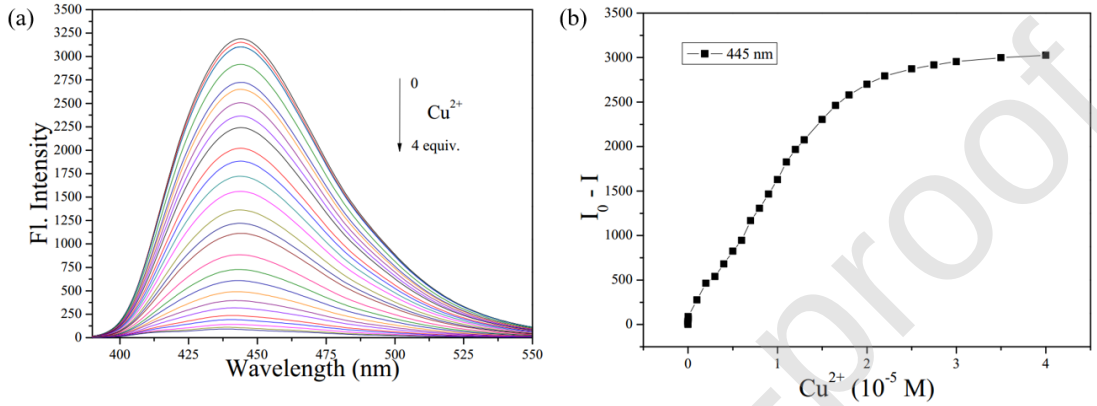

Fig. 6. Fluorescence emission spectra of **X**[Al^{3+}] upon gradually addition of Cu^{2+} (0 to 10 equiv.) in methanol/H_2O buffer solution (v/v = 9/1, tris = 10 mM, pH = 5.0).

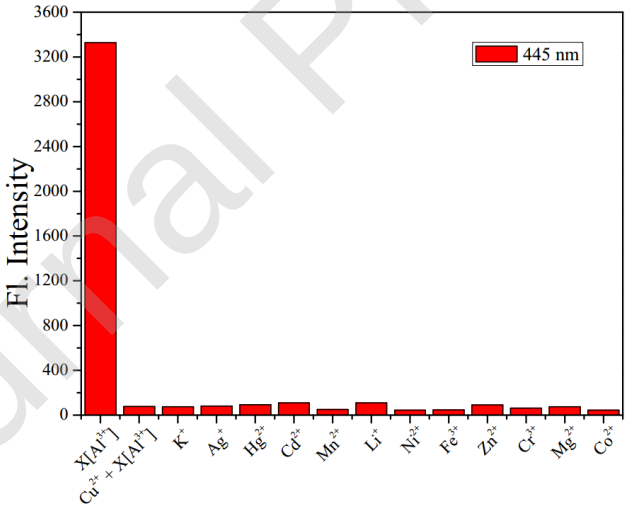

Fig. 7. Fluorescence intensity of **X**[Al^{3+}] in the presence of Cu^{2+} (3 equiv.) and followed by 3 equiv. of various other metal ions (K^+, Ag^+, Hg^{2+}, Cd^{2+}, Mn^{2+}, Li^+, Ni^{2+}, Fe^{3+}, Zn^{2+}, Cr^{3+}, Mg^{2+} and Co^{2+}) in methanol/H_2O buffer solution (v/v = 9/1, tris = 10 mM, pH = 5.0).

3.6. The effect of pH

The pH effect on the optical behavior of **X**, **X**[Al^{3+}] and **X**[Cu^{2+}] was investigated at different

pH varying from 2 to 12. As shown in Fig. 8, The fluorescence intensity of **X** remained constant at different pH values. Upon addition of Al^{3+} (10 equiv.), no change in fluorescence intensity was witnessed in basic conditions (pH **>** 8) which may be attributed to the hydrolysis behavior of Al^{3+} to form $Al(OH)_3$ and reduced the concentration of **X**[Al^{3+}]. Under acidic conditions (pH **<** 5), **X** exhibited an efficient sensing capability for Al^{3+} because the hydrolysis behavior of Al^{3+} was inhibited under acidic conditions resulting in the **X** being able to bind Al^{3+} more easily. When addition of Cu^{2+} (5 equiv.) to the system in the presence of Al^{3+}, the fluorescence intensity was completely quenched at different pH values. The investigated results suggested that under acidic conditions, **X** could be used as a sensor for detection of Al^{3+} and the complex **X**[Al^{3+}] further could act as a new sensor for Cu^{2+}, which provides the possibility to detect Al^{3+} and Cu^{2+} under extreme conditions [13, 46].

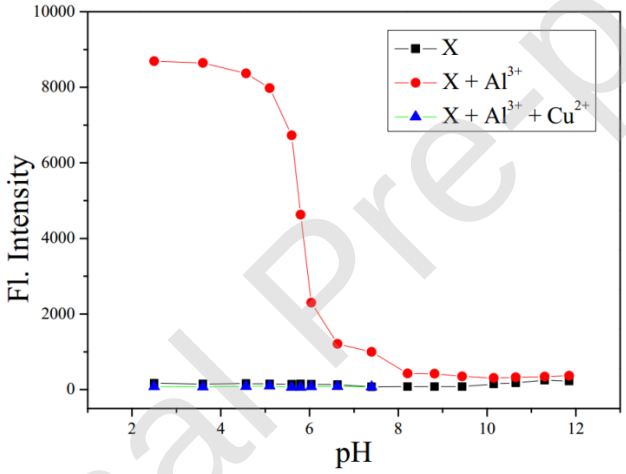

Fig. 8. The influence of pH value of solution on the fluorescence of **X**, **X**[Al^{3+}] and **X**[Cu^{2+}] in methanol/H_2O buffer solution.

3.7. The mechanism of binding mode and theoretical calculation

In order to clearly understand the **X** sensing mechanism for Al^{3+} and Cu^{2+}, the possible binding mechanisms were proposed based on based on fluorescence and mass spectrometry titration experiments [39, 40]. As shown in scheme 2, **X** exhibited weak fluorescence based on the PET mechanism and apparently formed a cavity to provide a complexation site for metal ions. After binding with Al^{3+}, the fluorescence intensity was significantly enhanced because the synergistic effect of PET and CHEF. Obviously, **X** binding to Al^{3+} through three coordination sites N (imidazole), N (C=N bond) and O (phenolic hydroxyl). When addition of Cu^{2+} to the system **X**[Al^{3+}],

Cu^{2+} could replace Al^{3+} in the original position and form a stable complex with **X** because Cu^{2+} had a stronger coordination ability than Al^{3+}. Cu^{2+} was a paramagnetic metal ion and could strongly quench the fluorescence intensity [35, 50]. So, the fluorescence disappeared again when Cu^{2+} were added.

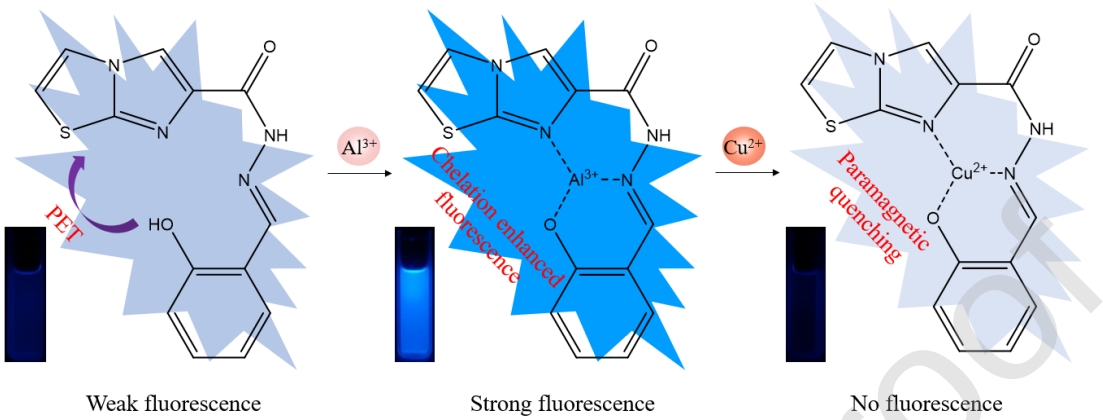

Scheme 2. The proposed binding mode of **X** with Al^{3+} and Cu^{2+}.

To better understand the sensing mechanism of **X** on Al^{3+} and Cu^{2+}, The optimized geometry and energy calculations of **X**, **X**[Al^{3+}] and **X**[Cu^{2+}] were investigated using *ab initio* density functional theory (DFT) combined with time-dependent density functional theory (TD-DFT), as implemented in the Gaussian 09 package based on the B3LYP/LANL2DZ basis set (for transition metal ion Cu^{2+}) and B3LYP/6-31G(d) basis set (for all the other elements) [30]. The optimized geometry of **X**, **X**[Al^{3+}] and **X**[Cu^{2+}] were presented in Fig. 9. For **X**, the imidazo[2, 1-*b*]thiazole and phenolic hydroxyl of **X** were in the same plane, which made the whole sensor molecule showed good coplanarity and stability. Moreover, it is highly consistent with the optimal structure proposed previously, which was conducive to coordination with metal ions. For **X**[Al^{3+}] and **X**[Cu^{2+}], a three-coordinate complex were formed between **X** and Al^{3+} or Cu^{2+}, including Al^{3+}-N (imidazole, 1.82 Å), Al^{3+}-N (C=N bond, 1.84 Å), Al^{3+}-O (phenolic hydroxyl, 1.68 Å) and Cu^{2+}-N (imidazole, 1.92 Å), Cu^{2+}-N (C=N bond, 2.04 Å), Cu^{2+}-O (phenolic hydroxyl, 1.84 Å), respectively. Obviously, the overall structure of sensor did not change significantly before and after binding metal ions.

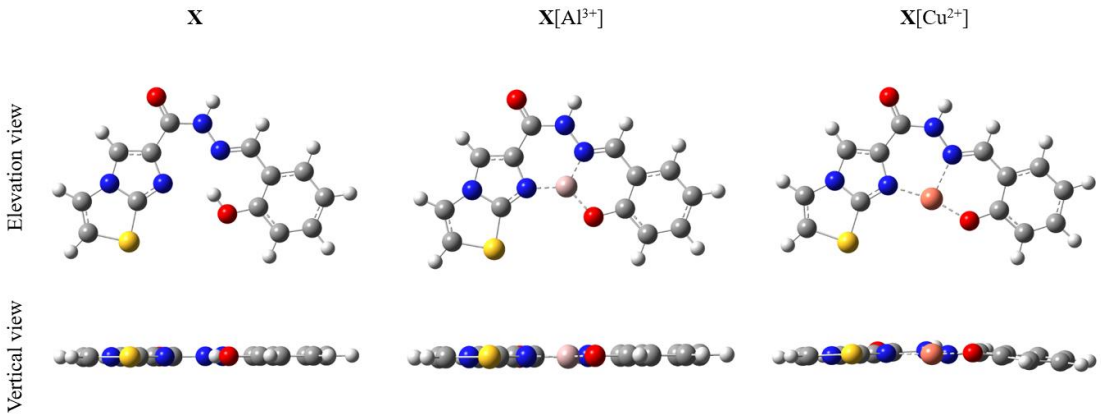

Fig. 9. The optimized geometry of **X**, **X**[Al^{3+}] and **X**[Cu^{2+}].

Moreover, the spatial distributions and orbital energies of the highest occupied molecular orbital (HOMO) and the lowest unoccupied molecular orbital (LUMO) were shown in Fig. 10. In the molecular orbital structure of **X**, the LUMO electron densities were mostly distributed in the phenol group and C=N bond while that of the HOMO electron densities spread on the whole **X**. The electrons were partially transferred under photon excitation, which implied a photoinduced electron transfer (PET) process. As a result, **X** displayed a weak fluorescence intensity. As for **X**[Al^{3+}], the HOMO and LUMO were mainly located near the Al^{3+} and on the benzene ring, indicating that the electron basically did not transfer in the excited state. So, the **X**[Al^{3+}] showed strong fluorescence due to the inhibition of PET process along with the CHEF mechanism [41]. As for **X**[Cu^{2+}], the HOMO and LUMO of **X**[Cu^{2+}] were similar to that of the **X**, but the electron transfer was not obvious. Moreover, the energy gap between HOMO and LUMO of **X**, **X**[Al^{3+}] and **X**[Cu^{2+}] were calculated to be 4.15 eV, 3.35 eV and 3.91 eV. After binding with metal ions (Al^{3+} and Cu^{2+}), the HOMO-LUMO energy gap became reduced, indicating the formation of a stable complex. Therefore, the calculated results were highly consistent with the experimental results and phenomena, proving that the binding mode and response mechanism proposed above were feasible and acceptable.

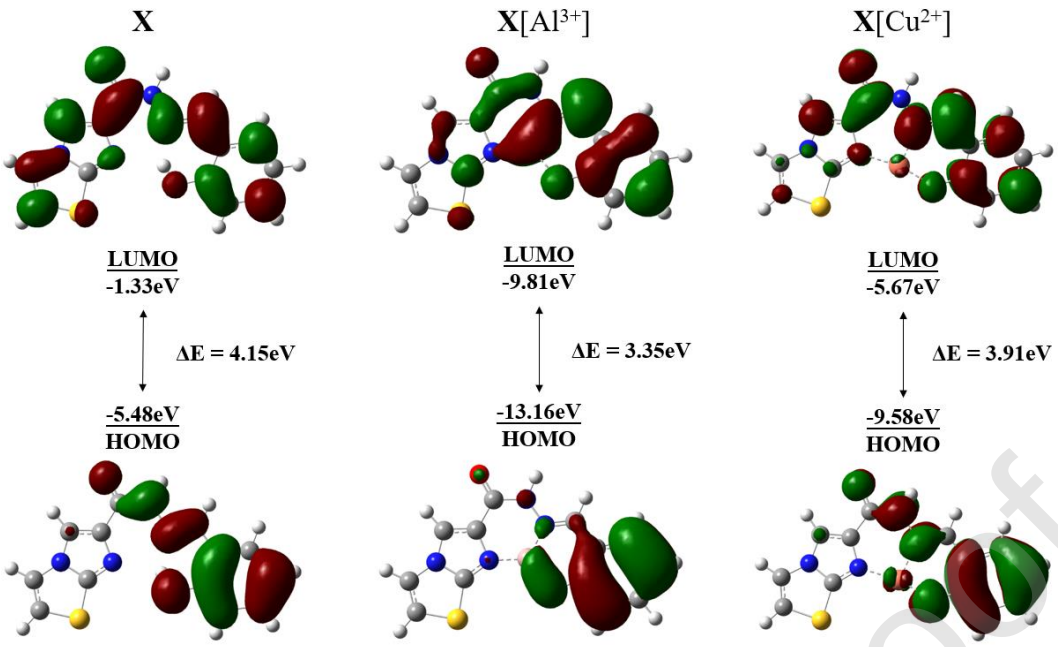

Fig. 10. The HOMO and LUMO of **X**, **X**[Al^{3+}] and **X**[Cu^{2+}].

3.8. Application in real water samples

To further investigate practical application of **X**, the amounts of Al^{3+} and Cu^{2+} in tap water were analyzed by proposed fluorescent method. The samples of Al^{3+} and Cu^{2+} with different concentration were prepared with tap water. In order to obtain a good experimental with a small deviation, all the measurements were performed three times. As shown in Table 1, a good agreement was obtained between the added and recovered ion amounts. The recovery value for Al^{3+} and Cu^{2+} were found in the range of 91.4% - 106.4% and 105.5% - 107.1%, respectively. And the relative standard deviation (RSD) of three measurements for Al^{3+} and Cu^{2+} was less than 1.91%, indicating that the measured data were reliable. In a word, a satisfactory recovery and RSD values were obtained, indicating that **X** could be used as a practical sensor to quantitatively detect Al^{3+} and Cu^{2+} in real water samples.

Table 1. Determination of Al^{3+} and Cu^{2+} in tap samples

Ion	Sample	Ion added (M)	Ion recovered (M)	Recovery (%)	RSD (%)
Al^{3+}	1	1.0×10^{-5}	1.06×10^{-5}	106.4	1.22
	2	3.0×10^{-5}	2.98×10^{-5}	99.5	0.91
	3	5.0×10^{-5}	4.57×10^{-5}	91.4	0.66
Cu^{2+}	1	5.0×10^{-6}	5.35×10^{-6}	107.1	1.38
	2	1.0×10^{-5}	1.05×10^{-5}	105.5	1.91

Conclusions

In summary, A new simple Schiff base, (E)-N'-(2-hydroxybenzylidene)imidazo[2,1-b]thiazole-6-carbohydrazide (**X**), was designed and synthesized based on salicylaldehyde and imidazo[2, 1-*b*]thiazole. The structure of **X** was characterized by ^{1}H NMR, ^{13}C NMR, FTIR, ESI-MS. In the methanol solution, **X** could be used as a sensor to identify Al^{3+} through a significant fluorescence enhancement at 445 nm with distinct color change from colorless to bright blue under UV light. And the complex **X**[Al^{3+}] could be used as a new sensor for Cu^{2+} through a highly efficient quenching behavior. Furthermore, the detection limits of sensor for Al^{3+} and Cu^{2+} were calculated to be 3.1×10^{-10} M and 9.8×10^{-11} M, respectively. Additionally, the association constants of **X**[Al^{3+}] and **X**[Cu^{2+}] were also determined to be 2.3×10^{4} M^{-1} and 6.1×10^{4} M^{-1}. In addition, the job's plot showed 1:1 stoichiometry between **X** and metal ions (Al^{3+} or Cu^{2+}). Otherwise, the optimized structure and energy calculations of **X**, **X**[Al^{3+}] and **X**[Cu^{2+}] were obtained by Gaussian 09 to prove the binding mode and sensing mechanism. And, the sensor successfully detected Al^{3+} and Cu^{2+} in the real water sample with a satisfactory recovery and RSD values, which provide a possibility for practical application.

Declaration of interests

The authors declare that they have no known competing financial interests or personal relationships that could have appeared to influence the work reported in this paper.

Yuankang Xu is studying for master degree in Department of Chemistry at University of Jinan. She received her BS in chemistry at University of Jinan in 2016.

Lei Yang is an employee of Henan Sanmenxia Aoke Chemical Industry Co. Ltd.

Hanyu Wang is studying for master degree in Department of Chemistry at University of Jinan.

Yanxia Zhang is a teacher in Department of Chemical Engineering, University of Jinan, China.

Xiaofeng Yang is an associate professor in Department of Chemical Engineering, University of Jinan, China. She received his Ph.D. degree in 2009 from Saitama University, her research focus is chemosensor based on small molecules.

Meishan Pei received his PhD degree in 2000 from Chinese Academy of Sciences. He is a professor in Department of Chemistry and Physics of Polymers. His current research focuses on functional polymer science.

Guangyou Zhang received his PhD degree in 1993 from Nanjing Forestry University. He is a professor in Department of Chemical Engineering, University of Jinan, China. His current research interests are mainly in the development of sensors for surfactants, metal ions, pharmaceutical anions, proteins and DNA based on fluorescent molecules.

All authors contribute equally.

Acknowledgements

The authors thank the Henan Sanmenxia Aoke Chemical Industry Co., Ltd. w0920 for financial support. Financial support by the National Natural Science Foundation of China (Grants 21708013) and the China Postdoctoral Science Foundation (Grants 2017M620288)

Reference

[1] Q. Wang, L. Yang, H. Wang, J. Song, H. Ding, X. Tang, H. Yao, A highly selective and sensitive turn- on fluorescent probe for the detection of Al^{3+} and its bioimaging, luminescence 32 (2016) 779-785.

[2] H. Chang, X. Zhao, W. Wu, L. Jia, Y. Wang, A highly sensitive on-off fluorescent chemosensor for Cu^{2+} based on coumarin, Journal of Luminescence 182 (2017) 268-273.

[3] T. Mandal, A. Hossain, A. Dhara, A. A. Masum, S. Konar, S. K. Manna, S. K. Seth, S. Pathak and S. Mukhopadhyay, Terpyridine derivatives as "turn-on" fluorescence chemosensors for the selective and sensitive detection of Zn^{2+} ions in solution and in live cells, Photochem. Photobiol. Sci. 17 (2018) 1068-1074.

[4] M. Rangasamy and K. Palaninathan, A pyrazoline-based fluorescent chemosensor for Al^{3+} ion detection and live cell imaging, New J. Chem. 42 (2018) 10891-10897.

[5] N. Li, S. Zeng, M. Li, Y. Ma, X. Sun, Z. Xing, J. Li, A Highly Selective Naphthalimide-Based Chemosensor: "Naked-Eye" Colorimetric and Fluorescent Turn-On Recognition of Al^{3+} and Its Application in Practical Samples, Test Paper and Logic Gate, Journal of Fluorescence 28 (2018) 347-357.

[6] K. Santhiya, S. K. Sen, R. Natarajan, R. Shankar and B. Murugesapandian, D-A-D Structured Bis-acylhydrazone Exhibiting Aggregation-Induced Emission, Mechanochromic Luminescence, and Al(III) Detection, J. Org. Chem. 83 (2018) 10770-10775.

[7] G. Bartwal, K. Aggarwal and J. M. Khurana, An ampyrone based azo dye as pH-responsive and chemo-reversible colorimetric fluorescent probe for Al^{3+} in semi-aqueous medium: implication towards logic gate analysis, New J. Chem. 42 (2018) 2224-2231.

[8] S. Suresh, N. Bhuvanesh, J. Prabhu, A. Thamilselvan, S. R. J. Rajkumar, K. Kannan, V. R. Kannan, R. Nandhakumar, Pyrene based chalcone as a reversible fluorescent chemosensor for Al^{3+} ion and its biological applications, Journal of Photochemistry and Photobiology A: Chemistry 359 (2018) 172-182.

[9] X. Yue, Z. Wang, C. Li, Z. Yang, A highly selective and sensitive fluorescent chemosensor and its application for rapid on-site detection of Al^{3+}, Spectrochimica Acta Part A: Molecular and

Biomolecular Spectroscopy 193 (2018) 415-421.

[10] B. Pang, C. Li, Z. Yang, Design of a colorimetric and turn-on fluorescent probe for the detection of Al(III), Journal of Photochemistry and Photobiology A: Chemistry 356 (2018) 159-165.

[11] T. Anand, A. K. S.K., S. K. Sahoo, A new Al^{3+} selective fluorescent turn-on sensor based on hydrazidenaphthalic anhydride conjugate and its application in live cells imaging, Spectrochimica Acta Part A: Molecular and Biomolecular Spectroscopy 204 (2018) 105-112.

[12] Q. Wang, X. Wen, Z. Fan, A Schiff base fluorescent chemsensor for the double detection of Al^{3+} and PPi through aggregation induced emission in environmental physiology, Journal of Photochemistry and Photobiology A: Chemistry 358 (2018) 92-99.

[13] M. Kumar, A. Kumar, M. S. H. Faizi, S. Kumar, M. K. Singh, S. K. Sahu, S. Kishor, R. P. John, A selective 'turn-on' fluorescent chemosensor for detection of Al^{3+} in aqueous medium: Experimental and theoretical studies, Sensors and Actuators B 260 (2018) 888-899.

[14] Y. Wang, Z. Ma, D. Zhang, J. Deng, X. Chen, C. Xie, X. Qiao, Q. Li, J. Xu, Highly selective and sensitive turn-on fluorescent sensor for detection of Al^{3+} based on quinoline-base Schiff base, Spectrochimica Acta Part A: Molecular and Biomolecular Spectroscopy 195 (2018) 157-164.

[15] S. Zeng, S. Li, X. Sun, M. Li, Y. Ma, Z. Xing, J. Li, A naphthalene-quinoline based chemosensor for fluorescent "turn-on" and absorbance-ratiometric detection of Al^{3+} and its application in cells imaging, Spectrochimica Acta Part A: Molecular and Biomolecular Spectroscopy 205 (2018) 276-286.

[16] Y. Jiao, L. Zhou, H. He, J. Yin, Q. Gao, J. Wei, C. Duan, X. Peng, A novel rhodamine B-based "off-on" fluorescent sensor for selective recognition of copper (II) ions, Talanta 184 (2018) 143-148.

[17] H. Ryu, M. G. Choi, E. J. Cho, S. Chang, Cu^{2+}-selective fluorescent probe based on the hydrolysis of semicarbazide derivative of 2-(2-aminophenyl)benzothiazole, Dyes and Pigments 149 (2018) 620-625.

[18] T. Sun, Q. Niu, T. Li, Z. Guo, H. Liu, A simple, reversible, colorimetric and water-soluble fluorescent chemosensor for the naked-eye detection of Cu^{2+} in ~ 100% aqueous media and application to real samples, Spectrochimica Acta Part A: Molecular and Biomolecular Spectroscopy 188 (2018) 411-417.

[19] N. Mergu, M. Kim, Y. Son, A coumarin-derived Cu^{2+}-fluorescent chemosensor and its direct application in aqueous media, Spectrochimica Acta Part A: Molecular and Biomolecular Spectroscopy 188 (2018) 571-580.

[20] G. He, X. Liu, J. Xu, L. Ji, L. Yang, A. Fan, S. Wang, Q. Wang, Synthesis and application of a highly selective copper ions fluorescent probe based on the coumarin group, Spectrochimica Acta Part A: Molecular and Biomolecular Spectroscopy 190 (2018) 116-120.

[21] L. Wang, Q. Bing, J. Li, G. Wang, A new "ON-OFF" fluorescent and colorimetric chemosensor based on 1,3,4-oxadiazole derivative for the detection of Cu^{2+} ions, Journal of Photochemistry and Photobiology A: Chemistry 360 (2018) 86-94.

[22] Q. Dai, H. Liu, C. Gao, W. Li, C. Zhu, C. Lin, Y. Tan, Z. Yuan and Y. Jiang, A one-step synthesized acridine-based fluorescent chemosensor for selective detection of copper(II) ions and living cell imaging, New J. Chem. 42 (2018) 613-618.

[23] Q. Bing, L. Wang, D. Li, G. Wang, A new high selective and sensitive turn-on fluorescent and ratiometric absorption chemosensor for Cu^{2+} based on benzimidazole in aqueous solution and its application in live cell, Spectrochimica Acta Part A: Molecular and Biomolecular Spectroscopy 202 (2018) 305-313.

[24] A. Ren, D. Zhu, W. Xie, X. He, Z. Duan, Y. Luo, X. Zhong, M. Song, X. Yan, A novel reaction-based fluorescent probe for sensitive and selective detection of Cu^{2+}, Inorganica Chimica Acta 476 (2018) 136-141.

[25] Y. Xia, H. Zhang, X. Zhu, G. Zhang, X. Yang, F. Li, X. Zhang, M. Fang, J. Yu, H. Zhou, A highly selective two-photon fluorescent chemosensor for tracking homocysteine via situ reaction, Dyes and Pigments 155 (2018) 159-163.

[26] H. Wang, B. Fang, L. Zhou, D. Li, L. Kong, K. Uvdal and Z. Hu, A reversible and highly selective two-photon fluorescent "on–off–on" probe for biological Cu^{2+} detection, Org. Biomol. Chem. 16 (2018) 2264-2268.

[27] Q. Wang, S. Wu, Y. Tan, Y. Yan, L. Guo, X. Tang, A highly selective, fast-response and fluorescent turn on chemosensor for the detection of Cu^{2+} ions and its potential applications, Journal of Photochemistry and Photobiology A: Chemistry 357 (2018) 149-155.

[28] L. Kang, Y. Liu, N. Li, Q. Dang, Z. Xing, J. Li, Y. Zhang, A schiff-base receptor based

naphthalimide derivative: Highly selective and colorimetric fluorescent turn-on sensor for Al^{3+}, Journal of Luminescence 186 (2017) 48-52.

[29] Y. Liu, F. Tian, X. Fan, F. Jiang, Y. Liu, Fabrication of an acylhydrazone based fluorescence probe for Al^{3+}, Sensors and Actuators B 240 (2017) 916-925.

[30] W. He and Z. Liu, A fluorescent sensor for Cu^{2+} and Fe^{3+} based on multiple mechanisms, RSC Adv. 6 (2016) 59073-59080.

[31] Y. Sie, C. Li, C. Wan, H. Yan, A. Wu, A novel fluorescence sensor for dual sensing of Hg^{2+} and Cu^{2+} ions, Journal of Photochemistry and Photobiology A: Chemistry 353 (2018) 19-25.

[32] D. Singhal, N. Gupta and A. K. Singh, Fluorescent sensor for Al^{3+} ion in partially aqueous media using julolidine based probe, New J. Chem. 40 (2016) 7536-7541.

[33] B. Pang, C. Li, Z. Yang, A novel chromone and rhodamine derivative as fluorescent probe for the detection of Zn(II) and Al(III) based on two different mechanisms, Spectrochimica Acta Part A: Molecular and Biomolecular Spectroscopy 204 (2018) 641-647.

[34] A. Ghosh and D. Das, X-ray structurally characterized sensors for ratiometric detection of Zn^{2+} and Al^{3+} in human breast cancer cells (MCF7): development of a binary logic gate as a molecular switch, Dalton Trans. 44 (2015) 11797-11804.

[35] J. Qin, Z. Yang, Fluorescent chemosensor for detection of Zn^{2+} and Cu^{2+} and its application in molecular logic gate, Journal of Photochemistry and Photobiology A: Chemistry 324 (2016) 152-158.

[36] Y. Fu, Y. Tu, C. Fan, C. Zheng, G. Liu and S. Pu, A highly sensitive fluorescent sensor for Al^{3+} and Zn^{2+} based on a diarylethene salicylhydrazide Schiff base derivative and its bioimaging in live cells, New J. Chem. 40 (2016) 8579-8586.

[37] X. Li, M. Yu, F. Yang, X. Liu, L. Wei and Z. Li, A dual-model and on–off fluorescent Al^{3+}/Cu^{2+}-chemosensor and the detection of F^-/Al^{3+} with 'in situ' prepared Al^{3+}/Cu^{2+} complexes, New J. Chem. 37 (2013) 2257-2260.

[38] S. B. Roy, K. K. Rajak, A quinoline appended naphthalene derivative based AIE active "turn–on" fluorescent probe for the selective recognition of Al^{3+} and colourimetric sensor for Cu^{2+}: Experimental and computational studies, Journal of Photochemistry and Photobiology A: Chemistry 332 (2017) 505-514.

[39] Y. Xu, H. Wang, J. Zhao, X. Yang, M Pei, G. Zhang, Y. Zhang, L. Lin, A simple fluorescent schiff base for sequential detection of Zn^{2+} and PPi based on imidazo[2,1-*b*]thiazole, Journal of Photochemistry and Photobiology A: Chemistry 383 (2019) 112026.

[40] Y. Xu, H. Wang, J. Zhao, X. Yang, M. Pei, G. Zhang and Y. Zhang, A dual functional fluorescent sensor for the detection of Al^{3+} and Zn^{2+} in different solvents, New J. Chem. 43 (2019) 14320-14326.

[41] P. Li, S. Xiao, A highly sensitive and selective sensor based on imidazo[1,2-a]pyridine for Al^{3+}, Journal of Photochemistry and Photobiology A: Chemistry 330 (2016) 169-174.

[42] S. Xiao, Z. Liu, J. Zhao, M. Pei, G. Zhang and W. He, A novel fluorescent sensor based on imidazo[1,2-a]pyridine for Zn^{2+}, RSC Adv. 6 (2016) 27119-27125.

[43] J. Sun, Z. Liu, Y. Wang, S. Xiao, M. Pei, X. Zhao and G. Zhang, A fluorescence chemosensor based on imidazo[1,2-a]quinoline for Al^{3+} and Zn^{2+} in respective solutions, RSC Adv. 5 (2015) 100873-100878.

[44] Y. Wu, F. Rahman, M. Z. Bhatti, S. Yu, B. Yang, H. Wang, Z. Li and D. Zhang, Acylhydrazone as a novel ‘‘Off–On–Off’’ fluorescence probe for the sequential detection of Al^{3+} and F^{-}, New J. Chem. 42 (2018) 14978-14985.

[45] W. Nasomphan, P. Tangboriboonrat, S. Smanmoo, Dansyl Based “Turn-On” Fluorescent Sensor for Cu^{2+} Ion Detection and the Application to Living Cell Imaging, J. Fluoresc. 27 (2017) 2201-2212.

[46] Y. Wang, Q. Meng, Q. Han, G. He, Y. Hu, H. Feng, H. Jia, R. Zhang and Z. Zhang, Selective and sensitive detection of cysteine in water and live cells using a coumarin-Cu^{2+} fluorescent ensemble, New J. Chem. 42 (2018) 15839-15846.

[47] X. Huang, K. Li, X. Wang, P. Xia, Rational design of an “on-off-on” fluorescent switch for Cu^{2+} and histidine based on chiral macrocyclic dioxopolyamine, Spectrochimica Acta Part A: Molecular and Biomolecular Spectroscopy 205 (2018) 287-291.

[48] S. Liu, Y. Liu, H. Pan, H. Chen, H. Li, Novel fluorescent probe bearing triarylimidazole and pyridine moieties for the rapid and naked-eye recognition of Cu^{2+}, Tetrahedron Letters 59 (2018) 108-112.

[49] S. B. Warrier, P. S. Kharkar, A coumarin based chemosensor for selective determination of Cu (II) ions based on fluorescence quenching, Journal of Luminescence 199 (2018) 407-415.

[50] L. Liu, F. Dan, W. Liu, X. Lu, Y. Han, S. Xiao, H. Lan, A high-contrast colorimetric and fluorescent probe for Cu^{2+} based on benzimidazole-quinoline, Sensors and Actuators B 247 (2017) 445-450.